Supplemental Figures – Fehniger et al.

Next-generation sequencing identifies the natural killer cell microRNA transcriptome

Figure S1. Schema of known miRNA expression analysis pipeline.

Figure S2. Filtered alignments comprising miRNA compressed sequences are mature miRNA in length.

Figure S3. Schema of novel miRNA gene analysis pipeline.

Figure S4. Analysis distribution of 1483 genomic clusters with read alignment depth > 50.

Figure S5. miR Validation tool screenshot.

Figure S6. NK cell miRNA detection is consistent across biological replicates.

Figure S7. Total miRNA abundance in resting and activated NK cells is similar assessed by real-time RT qPCR.

Figure S1

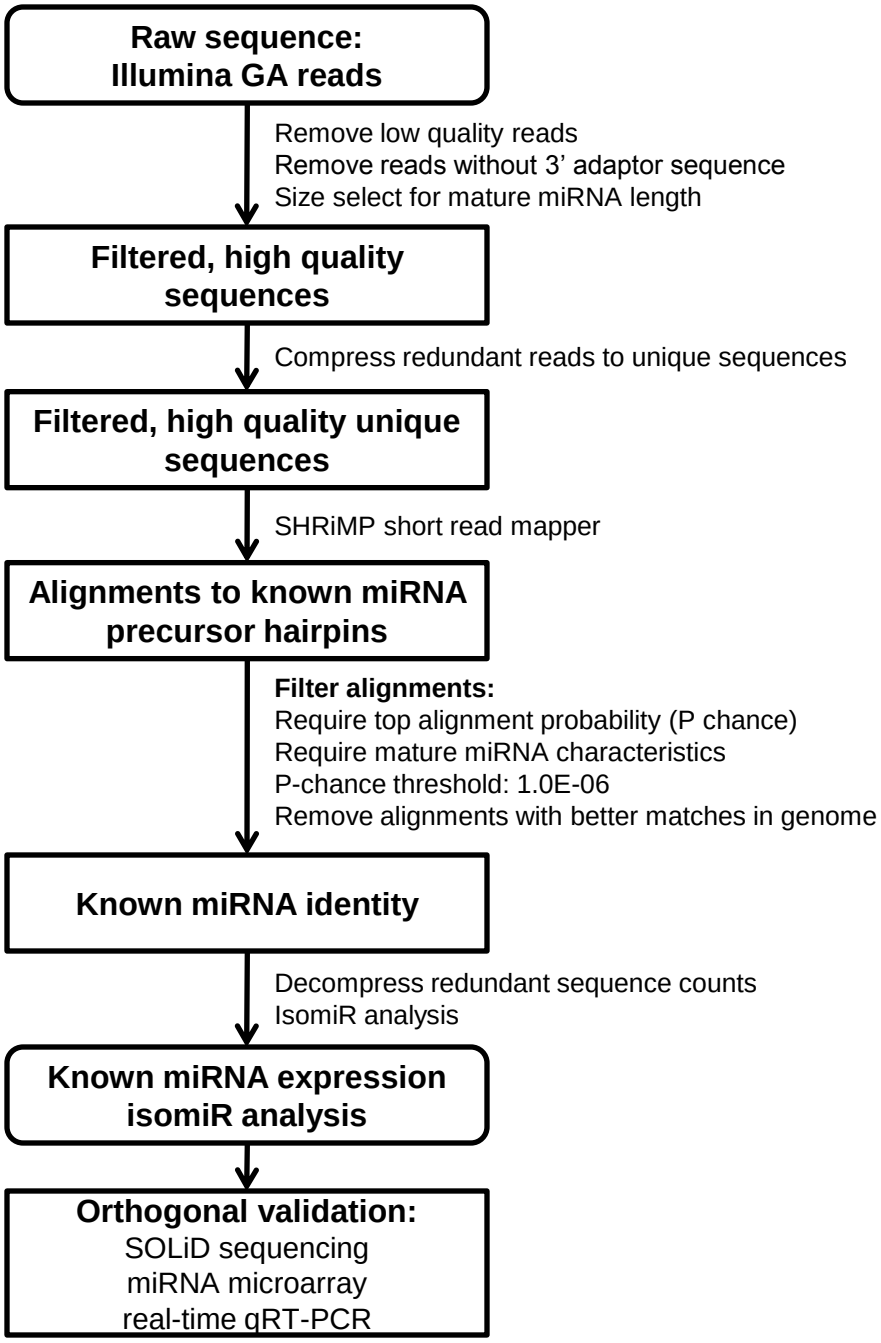

Figure S1. Schema of known miRNA expression analysis pipeline for Illumina GA sequencing.

Figure S2

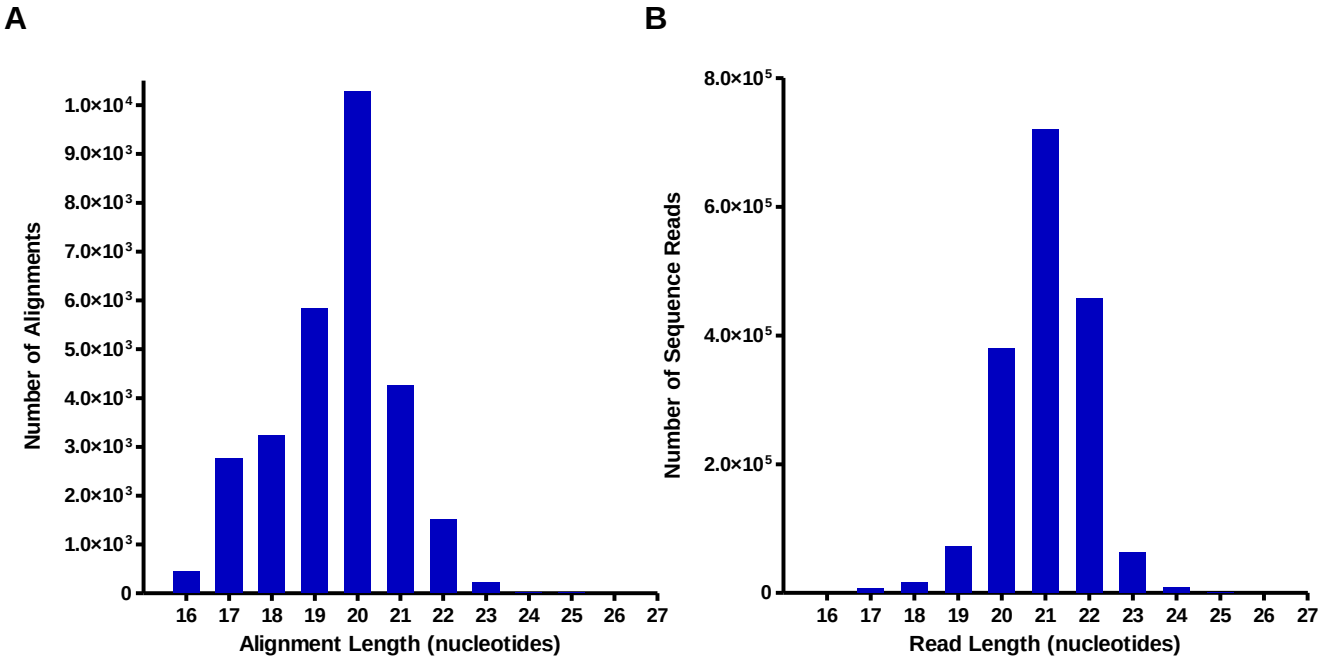

Figure S2. Filtered alignments comprising miRNA compressed sequences are mature miRNA in length. In order to verify that alignment parameters and filtered utilized for this analysis (Figure S1) resulted in mature miRNA length sequences and alignments, we analyzed the distribution of alignment and read length of all NK cell Illumina GA reads aligned to miRNA precursor hairpins and passing all filters. Shown are the alignment (A) and read (B) lengths for all sequence reads with identity to known miRNA.

Figure S3

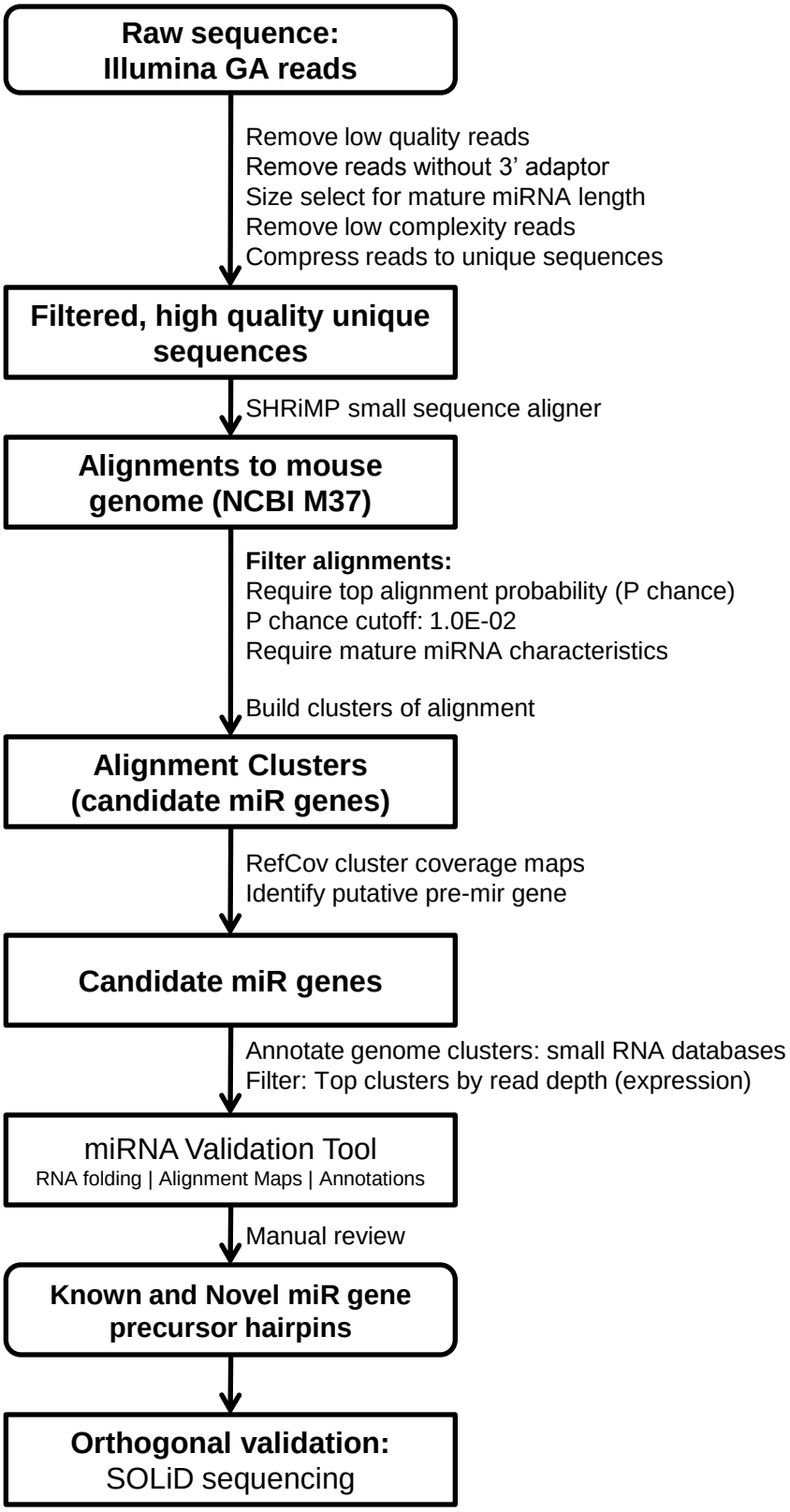

Figure S3. Schema of novel miRNA gene analysis pipeline.

Figure S4

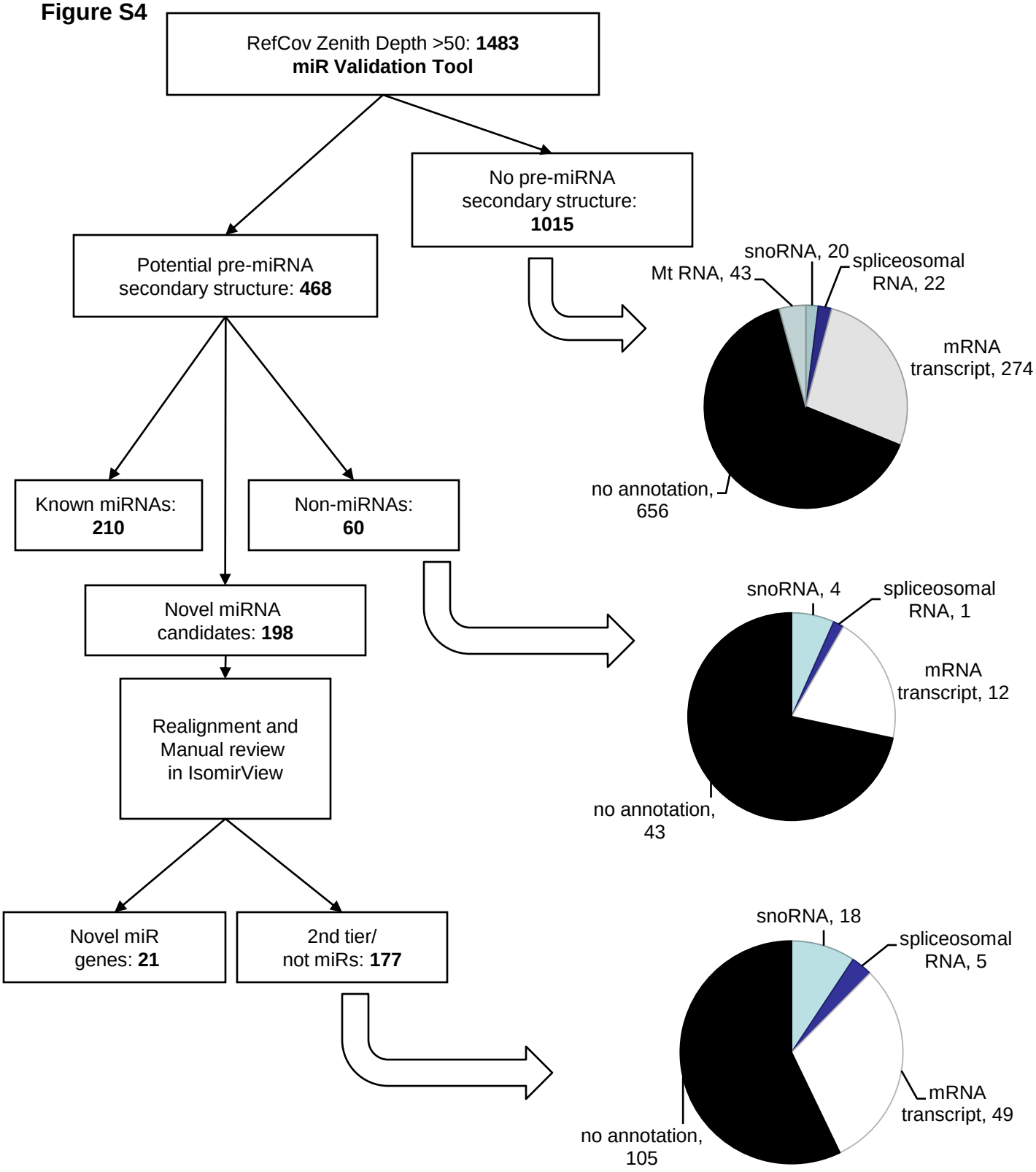

Figure S4. Analysis distribution of 1483 genomic clusters with read alignment depth of >50. Flow diagram showing the breakdown of genomic clusters evaluated as candidate novel miRNA genes. Pie charts show the annotations of indicated cluster bins.

Figure S5

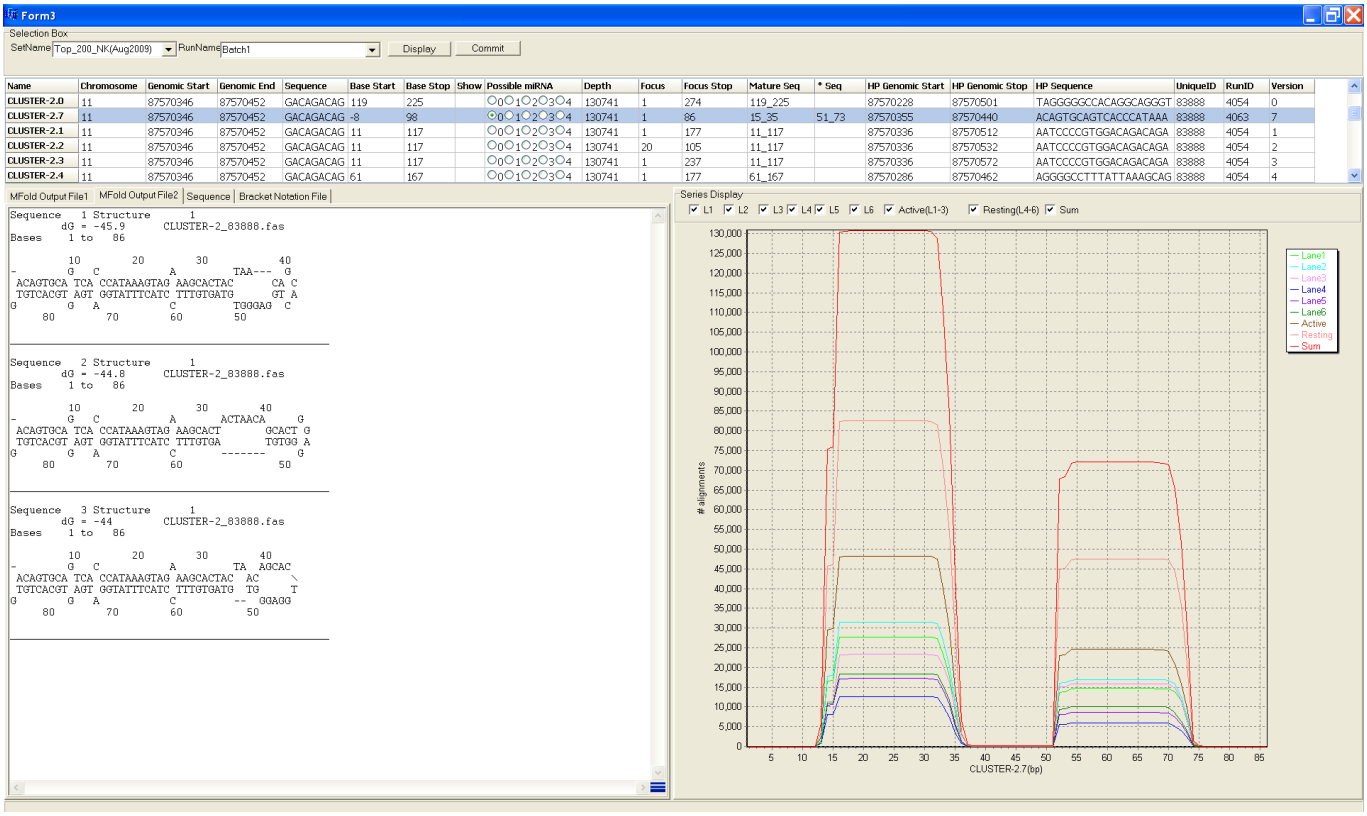

Figure S5. miR Validation tool screenshot. The in-house developed miR Validation tool (S Koul, R Nagarajan) displays genomic clusters with a summary table (top), Mfold secondary structure output (bottom left), and RefCov (T Wylie) based alignment coverage maps (bottom right). This example cluster, corresponding to miR-142, illustrates the miRNA precursor hairpin stem loop structure, and characteristic mature miRNA sequence alignment of NK cell Illumina GA reads in this case mapping to the 3p and 5p mature sequences.

Figure S6

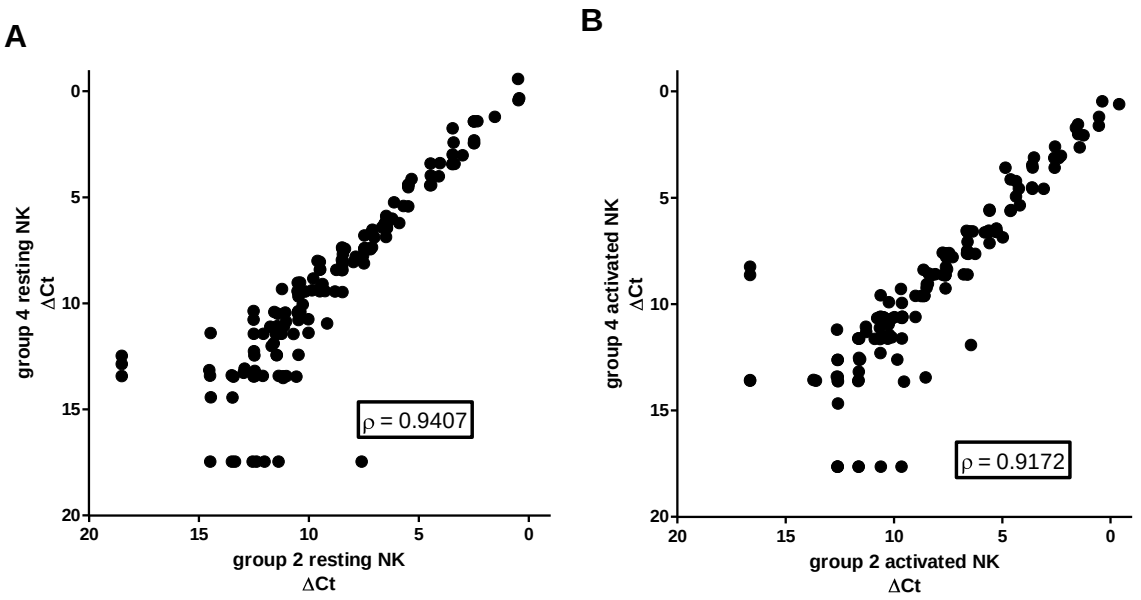

C

Resting NK

	G1	G2	G3	G4
G1				
G2	0.9447			
G3	0.9562	0.9419		
G4	0.9335	0.9407	0.9403	

Activated NK

	G1	G2	G3	G4
G1				
G2	0.9312			
G3	0.9077	0.8706		
G4	0.9138	0.9172	0.9345	

Figure S6. NK cell miRNA detection is consistent across biological replicates. Four biological replicates of resting and IL-15 activated NK cell pairs were analyzed for miRNA expression using ABI TaqMan RT qPCR array card A. Scatter plots of detected miRNAs (ΔCt, MammU6 control) in two resting (A) and activated (B) samples, demonstrating the consistency of miRNA expression and detection between replicates. Each circle represents an individual miRNA, and only primer/probe combinations that detected miRNAs in NK cells are included (ΔCt<15 for 3 of 4, or ΔCt<10 for 2 of 4). (C) Spearman's ρ was calculated for each replicate pair, and matrices for all four resting and activated NK cell biological replicates demonstrate high concordance.

Figure S7

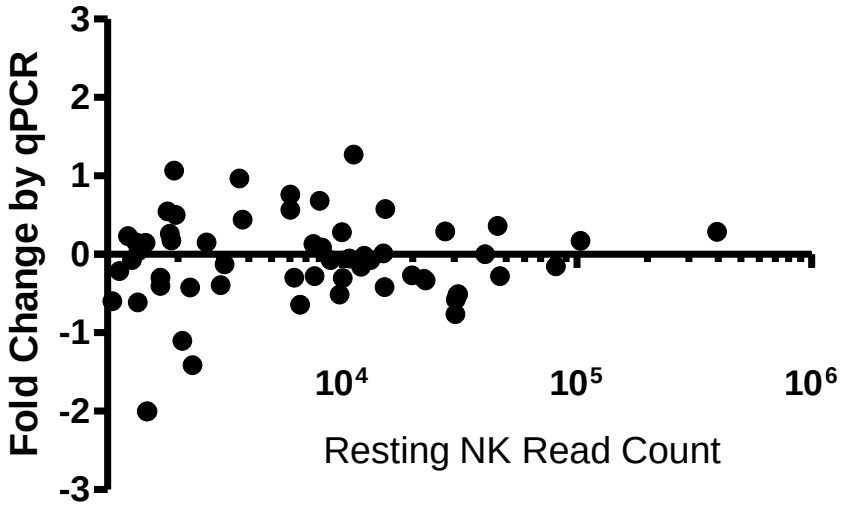

Figure S7. Total miRNA abundance in resting and activated NK cells is similar assessed by real-time RT qPCR. The most abundant miRNAs were plotted for absolute fold change between resting and activated NK cells samples (N=4 biological replicates, ΔCt method, MammU6 endogenous control) on the Y-axis, and their corresponding resting NK total read counts from Illumina on the X-axis. The miRNAs included in the analysis are those with >1000 read counts with RT qPCR primer/probes available, and represent 94.2% of all miRNA sequence reads. Minimal balanced fold changes were detected using qPCR for 94.2% of total miRNA content, suggesting that total miRNA abundance do not differ substantially between resting and activated NK cells in this study.